

The Casimir effect in the sphere-plane geometry

Antoine Canaguier-Durand

with Astrid Lambrecht, Serge Reynaud and Romain Guérout
Laboratoire Kastler-Brossel (CNRS, UPMC, ENS).

Collaborations with Paulo A. Maia Neto (Instituto de fisica UFRJ, Rio de Janeiro),
Gert-Ludwig Ingold (Institut für Physik, Universität Augsburg)
Valery V. Nesvizhevsky (Institute Laue-Langevin, Grenoble)
Alexei Yu. Voronin (P.N. Lebedev Physical Institute, Moscow)
and Ines Cavero-Peláez (Zaragoza University).



Laboratoire Kastler Brossel
Physique quantique et applications



Introduction

Motivation: study the non-trivial dependence of the Casimir interaction on the geometry.

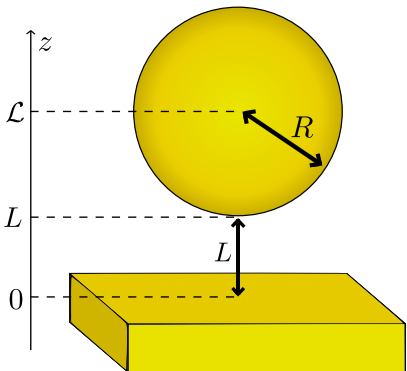
L : distance of closest approach.

R : radius of the sphere.

$$\mathcal{L} = L + R:$$

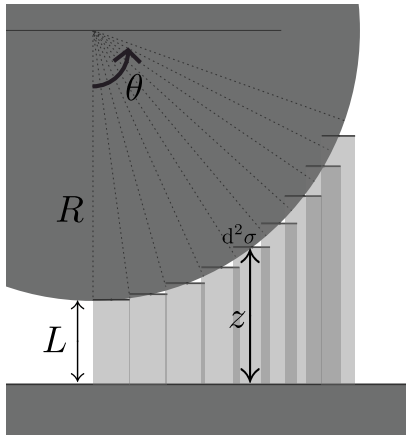
center-to-plate distance.

$$\frac{\mathcal{L}}{R}$$
: aspect ratio.



⇒ interesting geometry with curvature, non-specular reflection, coupling of polarizations, finite size (\neq plane-plane).

The Proximity Force Approximation (PFA)



$$F_{\text{PFA}} = 2\pi R \frac{E_{\text{PP}}}{A}$$

$$G_{\text{PFA}} = 2\pi R \frac{F_{\text{PP}}}{A}$$

Domain of validity is $(L \ll R)$ but the error is uncontrolled for $\frac{L}{R} > 0$.

$$\begin{aligned}\rho_E &= \frac{E}{E_{\text{PFA}}} \\ &= 1 + \beta_E \frac{L}{R} + \gamma_E \left(\frac{L}{R}\right)^2 + \dots\end{aligned}$$

- Estimation of the linear correction terms β_E , β_F and β_G (experimental prescription¹ $|\beta_G| < 0.4$).
- PFA uncouples geometry from other effects.

¹D.E. Krause, R.S. Decca, D. Lopez and E. Fishbach, *PRL* **8**, 243 (2007)

Plan

1 Method

- The scattering formalism
- Application to the sphere-plane geometry
- Numerical aspects

2 Zero temperature

- Perfect mirrors
- Metallic reflectors

3 Non-zero temperature

- Perfect mirrors
- Metallic reflectors

The scattering formula

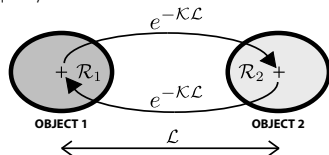
\mathcal{R} : Scattering operator

$$|\text{out}\rangle = \mathcal{R} |\text{in}\rangle$$

Round-trip operator ($\omega = i\xi$):

$$\mathcal{M}(i\xi) = \mathcal{R}_1(i\xi) e^{-\mathcal{K}\mathcal{L}} \mathcal{R}_2(i\xi) e^{-\mathcal{K}\mathcal{L}}$$

Scattering formula² at $T = 0$ and $T > 0$:



$$E = \frac{\hbar}{2\pi} \int_0^\infty d\xi \ln \det [\mathcal{I} - \mathcal{M}(i\xi)]$$

$$\mathcal{F} = k_B T \sum_n' \ln \det [\mathcal{I} - \mathcal{M}(i\xi_n)]$$

$$\text{with } \xi_n = n \frac{2\pi k_B T}{\hbar}$$

All information on geometry and optical properties is encoded in $\mathcal{M}(i\xi)$.

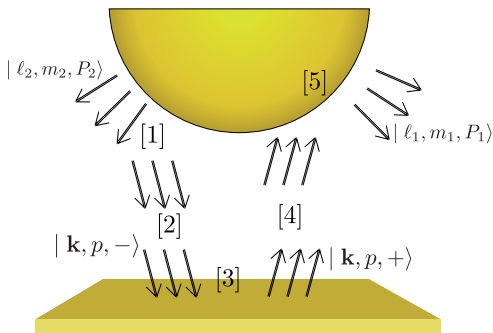
²A. Lambrecht, P.A. Maia Neto, and S. Reynaud, New J. Phys. **8**, 243 (2006).

Multipolar expansion in the sphere-plane geometry

$$\left\{ \begin{array}{l} \mathcal{F} = k_B T \sum'_n \ln \det(\mathcal{I} - \mathcal{M}(i\xi_n)) \quad ; \quad F = -\frac{\partial \mathcal{F}}{\partial L} \quad ; \quad G = \frac{\partial F}{\partial L} \\ \mathcal{M} = \mathcal{R}_S e^{-\mathcal{K}\mathcal{L}} \mathcal{R}_P e^{-\mathcal{K}\mathcal{L}} \quad ; \quad \xi_n = 2\pi n k_B T / \hbar \end{array} \right.$$

Multipolar expansion in the sphere-plane geometry

$$\left\{ \begin{array}{l} \mathcal{F} = k_B T \sum'_n \ln \det (\mathcal{I} - \mathcal{M}(i\xi_n)) ; \quad F = -\frac{\partial \mathcal{F}}{\partial L} ; \quad G = \frac{\partial F}{\partial L} \\ \mathcal{M} = \mathcal{R}_S e^{-\kappa \mathcal{L}} \mathcal{R}_P e^{-\kappa \mathcal{L}} ; \quad \xi_n = 2\pi n k_B T / \hbar \end{array} \right.$$



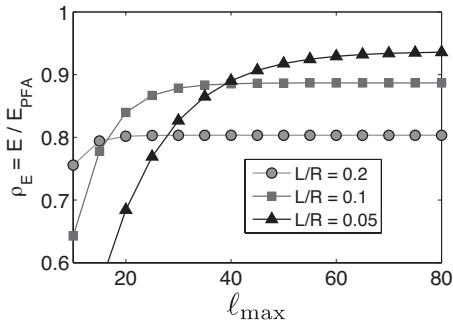
$$\mathcal{M}_{1;2} = \int \frac{d^2 \mathbf{k}}{(2\pi)^2} \sum_{p=TE,TM} \underbrace{\langle l_1 m_1 P_1 | \mathcal{R}_S | \mathbf{k}, +, p \rangle e^{-\kappa \mathcal{L}} r_p(k) e^{-\kappa \mathcal{L}}}_{\text{cavity operator}} \langle \mathbf{k}, -, p | l_2 m_2 P_2 \rangle$$

ℓ_{\max} cut-off

But numerics need $\dim(\mathcal{M}) < \infty$!

\Rightarrow truncation in the spherical modes at $|m| \leq \ell \leq \ell_{\max}$

- smaller $L/R \Rightarrow$ more modes ($\ell_{\max} \gtrsim \frac{4}{L/R}$ needed).
- for a given ℓ_{\max} , numerical results are accurate for large enough $\frac{L}{R}$.



- \Rightarrow Method well-adapted for $\frac{L}{R} \gtrsim 1$ (\rightarrow nanospheres³).
 \Rightarrow High truncation ℓ_{\max} allows for low values of $\frac{L}{R}$.

³A. Canaguier-Durand, A. Gérardin, R. Guérout, P. A. Maia Neto, V. Nesvizhevsky, Alexei Yu. Voronin, A. Lambrecht, S. Reynaud, *Phys. Rev. A* **83**, 032508 (2011).

Plan

1 Method

- The scattering formalism
- Application to the sphere-plane geometry
- Numerical aspects

2 Zero temperature

- Perfect mirrors
- Metallic reflectors

3 Non-zero temperature

- Perfect mirrors
- Metallic reflectors

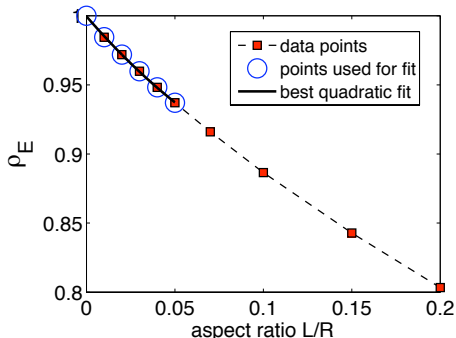
Comparison with the Proximity Force Approximation

Estimation of β :

$$\begin{aligned}\rho_E &= \frac{E}{E_{\text{PFA}}} \\ &= 1 + \beta_E \frac{L}{R} + \gamma_E \left(\frac{L}{R} \right)^2 + \dots\end{aligned}$$

\Rightarrow extrapolation to small $\frac{L}{R}$ in order to get the β_E .

From the fit, $\beta_E \simeq -1.47$ and $\beta_G = \frac{\beta_E}{3} = [-0.49]$.

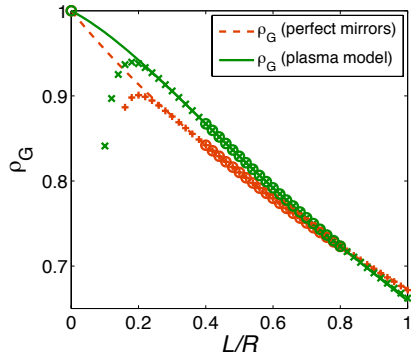


- Differs from scalar computations (8 times bigger) \Rightarrow coupling of polarizations.
- In contradiction with experimental $|\beta_G| < 0.4$ (Krause et al. 2007).
- In good agreement with other teams⁴.

⁴T. Emig, *J. Stat. Mech.: Theory Exp.*, P04007 (2008).

Influence of the material on the accuracy of PFA

Same procedure with plasma model⁵ for the mirrors $\rho_G = \frac{G_{\text{plas}}}{G_{\text{PFA}}}$:



- $R = 100 \text{ nm} ; \lambda_P = 136 \text{ nm}$.
- Accuracy of PFA is affected by imperfect reflection.
- Bending of the curve for ρ_G .
- $\beta_G^{\text{plas}} \simeq -0.2$ back inside the experimental bound.

⇒ Correlation between the effects of geometry and finite conductivity.

⁵A. Canaguier-Durand, P. A. Maia Neto, I. Cavero-Pelaez, A. Lambrecht, S. Reynaud, *Phys. Rev. Lett.* **102**, 230404 (2009).

Plan

1 Method

- The scattering formalism
- Application to the sphere-plane geometry
- Numerical aspects

2 Zero temperature

- Perfect mirrors
- Metallic reflectors

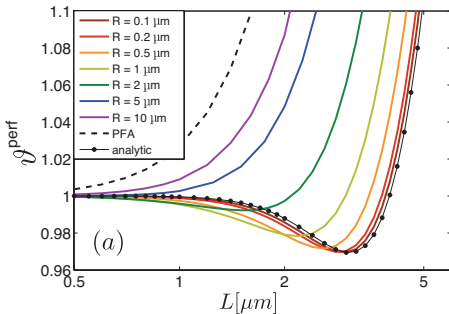
3 Non-zero temperature

- Perfect mirrors
- Metallic reflectors

Temperature and geometry (1/2)

$(L, R, \lambda_T = \frac{\hbar c}{k_B T})$: inclusion of $T = 300$ K through the Matsubara sum.

Change in the Casimir force due to the temperature⁶ $\vartheta = \frac{F(T)}{F(0)}$:



- $\vartheta < \vartheta_{\text{PFA}}$: lower thermal increase.
- depends on R .
- convergence to analytical result ($R \ll L$).
- $\vartheta_F < 1$: repulsive contribution of thermal photons to the force.

⇒ Correlations between the effects of geometry and temperature (already observed for scalar fields⁷).

⁶A. Canaguier-Durand, P. A. Maia Neto, A. Lambrecht, S. Reynaud, *Phys. Rev. Lett.* **104**, 040403 (2010).

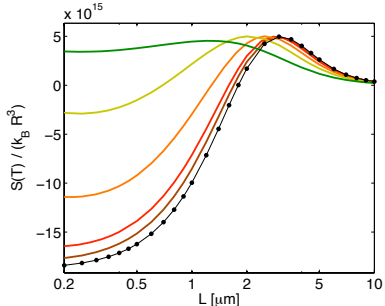
⁷K. Klingmüller and H. Gies, *J. Phys. A* **41** 164042 (2008).

Temperature and geometry (2/2)

- ($L \gg R$)-limit can be computed analytically for any temperature:

$$\mathcal{F}^{perf} \simeq -\frac{3\hbar cR^3}{4\lambda_T \mathcal{L}^3} \phi(\nu) \quad \text{with} \quad \begin{cases} \phi(\nu) &= \frac{\nu^2 \cosh \nu + \nu \sinh \nu + \cosh \nu \sinh^2 \nu}{2 \sinh^3 \nu} \\ \nu &= 2\pi \frac{\mathcal{L}}{\lambda_T} \end{cases}$$

- its ($T \rightarrow 0$)-limit in agreement with corresponding limit in a different derivation⁸.
- $\vartheta < 1$ can be related to the appearance of negative values for the Casimir entropy⁹ $S = -\frac{\partial \mathcal{F}}{\partial L}$.

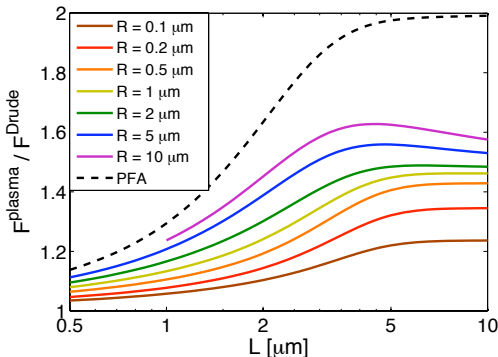


⁸M. Bordag, I. Pirozhenko, *Phys. Rev. D* **81** 085023 (2010).

⁹A. Canaguier-Durand, P.A. Maia Neto, A. Lambrecht, S. Reynaud, *Phys. Rev. A* **82**, 012511 (2010).

Interplay between the effect of dissipation and geometry

We compare the results of plasma and Drude models by taking the ratio $\frac{F_{\text{plasma}}}{F_{\text{Drude}}}$ at non-zero temperature.



- strong interplay between geometry, temperature and dissipation.
- the gap between plasma and Drude is always smaller.
- large distance analytical limit:

$$\frac{F_{\text{plasma}}}{F_{\text{Drude}}} (L \rightarrow \infty) \leq \frac{3}{2}$$

Conclusions

Scattering formalism allows to treat exactly the sphere-plane geometry, with a full EM multipolar treatment.

The sphere-plane configuration is a simple example to study the dependance of the Casimir effect on the geometry:

- coupling of the polarizations \Rightarrow full EM treatment necessary.
- correlations between the geometry and the effects of finite conductivity $\Rightarrow \beta_G$ is no more in contradiction with experimental prescription.
- correlations between the geometry and temperature \Rightarrow temperature can reduce $|F|$.
- correlations between the geometry and the effects of dissipation and temperature $\Rightarrow \frac{F_{\text{plas}}}{F_{\text{Drud}}} \leq \frac{3}{2}$ at large distances (instead of 2 for plane-plane).